Translational Oncology 66 (2026) 102722

Contents lists available at ScienceDirect

Translational Oncology

journal homepage: www.elsevier.com/locate/tranon

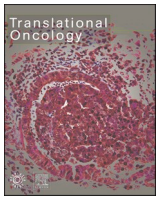

Single-cell analysis of TIGD genes in hepatocellular carcinoma: Prognostic value and functional characterization

Jing Liu [a,1], Xiaopeng Chen [a,b,1], Cheng Liu [c,1], Chengwei Yang [a,b], Baoding Li [a,*]

[a] Department of Hepatobiliary Surgery, People's Hospital of Ningxia Hui Autonomous Region, Ningxia Medical University, Yinchuan, Ningxia, 750000, China
[b] Third Clinical Medical College, Ningxia Medical University, Yinchuan, Ningxia, 750000, China
[c] Clinical laboratory, The Third Affiliated Hospital of Sun Yat-Sen University, Guangzhou, 510630, China

ARTICLE INFO

Keywords:
Hepatocellular carcinoma
TCGA
TIGD
Prognosis
Stem cell

ABSTRACT

Background: Hepatocellular carcinoma (HCC) is an aggressive cancer with limited therapies. Although transposable element–derived genes are increasingly linked to tumorigenesis, the role of the TIGD family in HCC remains unclear. This study examined the expression, clinical significance, and stemness-related features of TIGDs in HCC, emphasizing their prognostic and therapeutic potential.

Method: TIGD expression was analyzed using TCGA data via GEPIA2, cBioPortal, and Kaplan–Meier Plotter, with protein validation from the Human Protein Atlas. Single-cell RNA-seq data (GSE242889) were used to examine TIGD expression across hepatic cell types. Survival and Cox regression analyses assessed prognostic value, while functional enrichment and immune infiltration analyses explored biological roles. TIGD5-high and TIGD5-low epithelial subsets were compared for functional features and cell–cell communication.

Results: TIGD1, 3, 4, 5, 6, and 7 were significantly upregulated in HCC. High TIGD4, TIGD5, and TIGD6 expression correlated with poorer overall survival and served as independent prognostic markers. TIGD5 exhibited the broadest and highest expression across immune and stromal compartments. Stratification of epithelial cells into TIGD5-high and TIGD5-low subsets revealed distinct functional phenotypes: TIGD5-high cells showed enrichment in extracellular matrix organization, growth factor signaling, and immune regulatory pathways, with enhanced communication probability within the tumor microenvironment. Notably, TIGD5+ epithelial cells demonstrated increased interaction strength and MIF signaling pathway engagement compared to TIGD5- counterparts. Functional analyses indicated roles in RNA splicing, DNA replication, and cell-cycle regulation. TIGDs also showed associations with immune infiltration, particularly Th2 cells.

Conclusion: TIGD4, TIGD5, and TIGD6 exhibit oncogenic potential and may serve as prognostic biomarkers and therapeutic targets in HCC. Their stem-cell–associated expression highlights a novel connection between transposable element-derived genes and liver cancer stemness.

Introduction

Liver cancer, a primary malignancy of the liver, ranks among the most common causes of cancer-associated mortality on a global scale [1, 2]. Hepatocellular carcinoma (HCC), which accounts for approximately 75 %−85 % of liver cancer cases globally, is the predominant type of primary liver cancers [3–7]. Hepatocellular carcinoma has numerous risk factors, including hepatitis B and C infections, chronic alcohol use, aflatoxin exposure, autoimmune hepatitis, obesity, and diabetes [8–11]. Despite recent progress in understanding the molecular mechanisms underlying hepatocarcinogenesis, the translation of this knowledge into effective targeted therapies and improved clinical outcomes remains limited. Consequently, it is crucial to identify new specific molecular markers for diagnosing and predicting HCC, which could aid in creating targeted diagnostic and treatment approaches.

TIGD1–7, or Tigger transposable element derived 1–7, is part of the Tigger subfamily within the Pogo superfamily of human DNA-mediated transposons [12]. POGO transposons have an evolutionary background in eukaryotes and have been repeatedly domesticated in vertebrates. TIGD3, TIGD4, and TIGD5 are likely indicative of early domestication occurrences in vertebrates, while TIGD2, TIGD6, and TIGD7 seem to signify the latest domestication events in mammals [13]. Accumulating

* Corresponding author.
E-mail address: libaoding132@163.com (B. Li).
[1] Jing Liu, Xiaopeng Chen and Cheng Liu are co-first authors.

https://doi.org/10.1016/j.tranon.2026.102722
Received 6 December 2025; Received in revised form 14 February 2026; Accepted 26 February 2026

evidence indicates that transposable element-derived genes are frequently reactivated in cancer and contribute to oncogenesis through diverse mechanisms, including genome instability, epigenetic dysregulation, and activation of oncogenic signaling pathways. TIGD1, a unique gene of human species, is a differential expression gene -related differential expression gene during the formation of liver cancer. TIGD1 is highly expressed in eight types of tumor tissues, including brain and central nervous system cancer, breast cancer, colorectal cancer, gastric cancer, head and neck cancer, liver cancer, lung cancer, and pancreatic cancer, compared to normal tissue [14]. Xiaoqin [15] discovered that TIGD1 is highly expressed in Adrenocortical carcinoma and correlates with a poor prognosis for patients, as revealed by bioinformatics. While TIGD2 itself remains functionally uncharacterized, transposable element-derived genes (including other TIGD family members) have been implicated in regulating cell identity and lineage specification. For example, the domestication of transposable elements has given rise to genes essential for placental development (e.g., syncytin genes derived from endogenous retroviruses) and neuronal diversification. Analysis of GTEx data reveals that TIGD2 exhibits predominant expression in the cerebellum with minimal expression in the substantia nigra [16]. TIGD3 is a gene encoding DNA conversion element. There is a significant correlation between TIGD3 expression and the levels of polychlorinated biphenyls in blood or urine, as well as 1-hydroxypyrene in urine [17]. TIGD4 exhibits differential expression patterns between lymph node and brain metastases in breast cancer, with significantly higher levels observed in brain metastases compared to lymph node metastases. In vitro functional studies demonstrate that TIGD4 overexpression enhances breast cancer cell migration and invasion, while TIGD4 knockdown suppresses these metastatic behaviors [18,19]. Specifically, elevated TIGD4 promotes epithelial-mesenchymal transition (EMT) and increases matrix metalloproteinase (MMP) activity, facilitating tumor cell dissemination to distant organs. TIGD5 is a risk gene closely related to autism spectrum disorder (ASD). Xinyan Xie [20] employed the convergent functional genomics (CFG) approach to identify TIGD5 as linked to a higher risk of ASD. The expression of TIGD6 is detected in many tissues, which may differ in expression between obese and non-obese individuals [21]. TIGD7, expressing in a wide variety of tissues, has been implicated in cardiovascular disease, fat metabolism or related health traits [22,23]. Thus far, there are only a limited number of studies on the diagnostic and prognostic importance of TIGDs in HCC. The exact function of TIGDs are unknown, and the molecular mechanisms remain poorly understood [24]. This research utilizes bioinformatics to examine the expression patterns of TIGDs and investigates their connections with clinical features, prognostic significance, immune cell infiltration, mutation status, and roles in HCC. We hoped that our work would aid in the development of early diagnosis and therapeutic options for HCC patients.

Materials and methods

Data acquisition

A cohort of 15,776 samples, comprising RNA-seq data and associated clinical information spanning 33 tumor types [25], was acquired from The Cancer Genome Atlas (TCGA) and the Genotype-Tissue Expression (GTEx) database via UCSC XENA. For the present analysis, RNA-Seq data from 374 HCC patients and 50 normal tissues—including gene expression profiles, immune infiltrate data, and relevant clinical records—were obtained from the TCGA hepatocellular carcinoma (HCC) cohort. Subsequently, Level 3 HTSeq-FPKM formatted data were converted to transcripts per million (TPM) to facilitate downstream analytical procedures [26].

Gene expression profiling interactive analysis 2 (GEPIA2)

GEPIA2 constitutes a comprehensive cancer genomic resource that amalgamates extensive datasets derived from The Cancer Genome Atlas (TCGA) and the Genotype-Tissue Expression Project (http://gepia2.cancer-pku.cn/#index) [27]. Associations of TIGDs with tumor stage were assessed using GEPIA2, with Pearson's correlation coefficient applied as the statistical measure. The "Similar Gene Detection" module (http://gepia2.cancer-pku.cn/#similar) was employed to pinpoint the 100 most analogous genes to members of the TIGD family.

Human protein atlas (HPA)

Data for the HCC and normal tissues plot were retrieved from the Human Protein Atlas (https://www.proteinatlas.org/) [28]. HPA applies transcriptome and proteomics to provide different protein maps, including tissue atlas, brain atlas, single cell atlas, tissue cell atlas and pathology atlas.

cBioPortal

Gene variant profiling of hepatocellular carcinoma (HCC), encompassing amplification, mutation, and copy number variation, was conducted employing cBioPortal (https://www.cbioportal.org/) [29,30]. This platform furnishes a synopsis of genetic modifications for individual TIGD family members, facilitating comprehensive visualization of all mutation categories within each sample.

Correlation analyses of TIGDs

To evaluate the relationships between pairs of TIGDs, Pearson's correlation coefficient was employed. All statistical computations and graphical representations were generated using R software (×64 4.2.1). A significance threshold of $p < 0.05$ was applied for statistical inferences.

Immune infiltration analysis

To investigate associations of TIGDs with 24 immune cell categories, single-sample gene set enrichment analysis (ssGSEA) was implemented through the GSVA package in R [31,32]. Furthermore, Spearman's correlation approach was utilized to examine relationships between TIGDs expression and immune checkpoint gene expression levels.

Survival analysis

HCC patients were stratified into two distinct cohorts according to TIGDs expression levels. To assess whether TIGDs expression influences clinical outcomes, a prognostic model was developed utilizing Kaplan-Meier (KM) survival analysis.

Analyses of univariate and multivariate Cox regression

The OS of two cohorts of patients with HCC and the expression level of TIGD4, 5, 6 were compared using univariate Cox regression analysis. Furthermore, we employed multivariate analysis to assess if TIGD4, 5, 6 serve as independent prognostic indicators for overall survival in patients with HCC. The survival package was utilized for statistical analysis.

Single-cell RNA sequencing data processing and analysis workflow

scRNA-seq data for human hepatocellular carcinoma (dataset GSE242889) were retrieved from the Gene Expression Omnibus (GEO) database. Quality control screening was applied to the raw count matrix employing the Seurat package (v5.2.1). Sequential removal was conducted for cells exhibiting fewer than 200 detected genes, over 5000 detected genes (indicative of doublets), or mitochondrial gene content exceeding 10 % of total counts. After quality control, normalization,

dimensionality reduction, and clustering were carried out using Seurat's standard pipeline. To reduce batch effects, Harmony (v1.2.3) was implemented on the top 2000 highly variable genes with default settings. Through systematic assessment, a clustering resolution of 0.1 was identified as optimal for subsequent visualization and analysis [33]. Initial cell type annotation involved manual consultation of liver-specific marker genes documented in the ACT database (http://xteam.xbio.top/ACT/index.jsp) [34,35]. Thereafter, the UCell algorithm was utilized for automated scoring of cells according to curated gene signatures for specific cell types, thereby ensuring consistency and cross-validation of annotations.

Quantitative real-time PCR (qRT-PCR) analysis

TRIZOL reagent (Thermo Fisher, USA) was used to extract total RNA. cDNA synthesis was carried out with the Hifair™ II 1st Strand cDNA Synthesis SuperMix Kit (YEASEN, Shanghai, China) following the manufacturer's instructions. Quantitative real-time PCR assays were conducted using ChamQ SYBR qPCR Master Mix (Vazyme, Nanjing, China) according to the provided protocol. For normalization of mRNA expression, S(Human) served as an endogenous control [30]. Sequences used in this study were listed as follows: TIGD4 forward (F): 5′-TGTACCAGTAGACCCTTCGAC-3′, TIGD4 reverse (R): 5′-AACATTCG ATAAAGCAGCCCA-3′; TIGD5 (F): 5′-CGCAAGGCCTACTCCATCAA-3′, TIGD5 (R): 5′-GCATCTTCTTGCGCTGAGTG-3′; TIGD6 (F): 5′-AGA AGCGTCGGCAGTTCTC-3′, TIGD6 (R): 5′- ACCAAGCAAAAACAGC CTTATCA-3′.

Statistical analysis

Statistical analyses of TCGA data were conducted with R software version 4.2.1. Expression levels of TIGDs in hepatocellular carcinoma (HCC) versus normal tissues were assessed using Wilcoxon rank-sum and signed-rank tests, with corresponding 95 % confidence intervals (CIs) provided [36]. Evaluation of receiver operating characteristic (ROC) curves for TIGDs was carried out via the pROC package. The resulting area under the curve (AUC) measurements varied between 0.5 and 1.0, demonstrating discriminatory power of 50 % to 100 %.

Results

Analysis of TIGDs mRNA expression levels in human cancer

Expression profiles of TIGD family members between malignant and matched normal tissues were evaluated using the TCGA and GTEx pan-cancer datasets (Fig. 1A). TIGDs expression was markedly increased across most cancer types within the TCGA repository relative to normal controls. TIGD1 mRNA exhibited differential expression in carcinomas versus adjacent tissues, with 22 malignancies showing up-regulation and 7 displaying down-regulation. For TIGD2, significant over-expression was observed in 21 tumor types, while under-expression occurred in 4 others. TIGD3 demonstrated pronounced up-regulation in 24 cancers and was down-regulated in 4 malignancies. TIGD4 was significantly elevated in 17 tumor types and reduced in 7 others. TIGD5 showed substantial up-regulation across 26 cancers. TIGD6 was over-expressed in 17 malignancies and under-expressed in 4, whereas TIGD7 was up-regulated in 11 tumor types and down-regulated in an equal

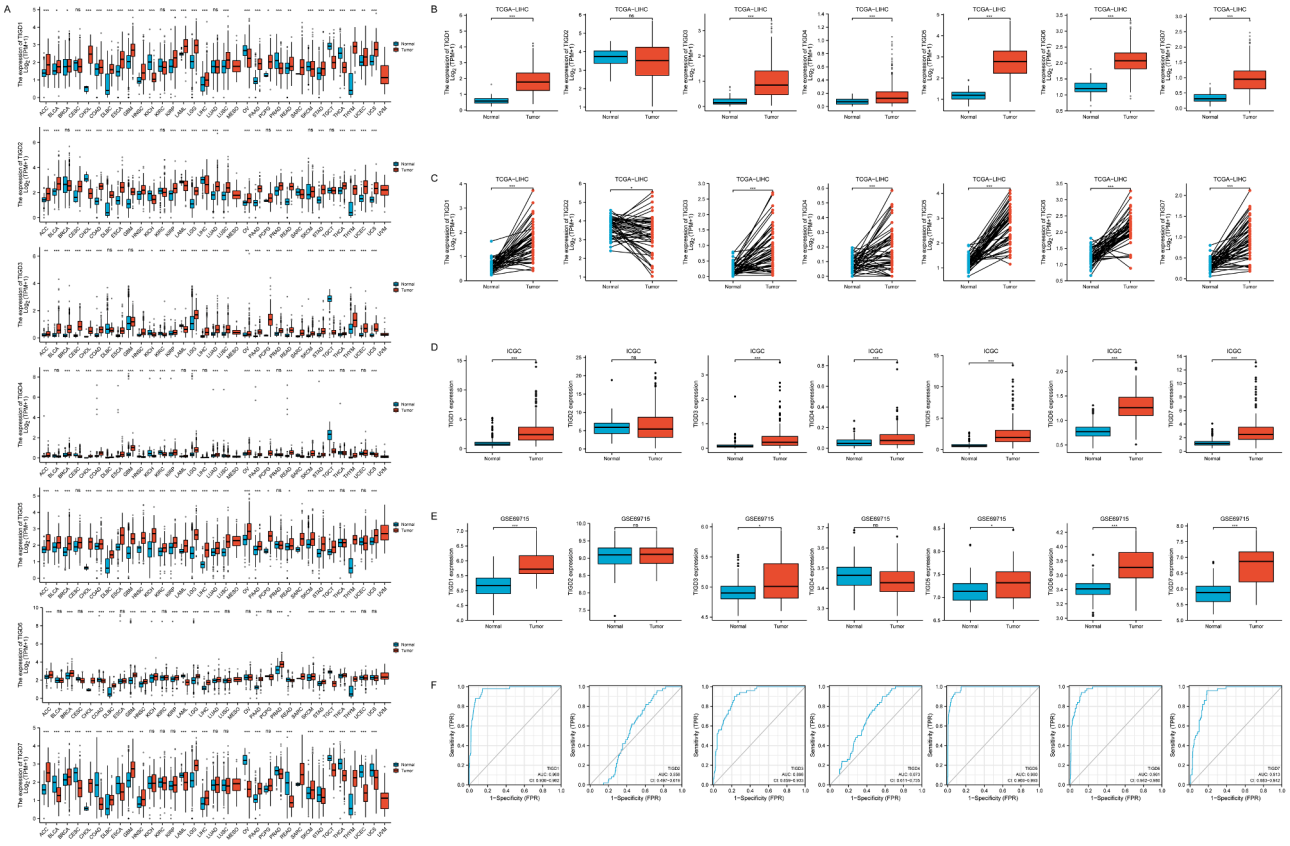

Fig. 1. illustrates the mRNA expression profiles of TIGDs across human malignancies. (A) Comparative expression of TIGDs in cancerous versus non-cancerous tissues based on pan-cancer data from The Cancer Genome Atlas (TCGA) and the Genotype-Tissue Expression (GTEx) project. (B) Expression levels of TIGDs in hepatocellular carcinoma (HCC) and matched normal liver tissues from the TCGA database. (C) Paired analysis of TIGDs expression in HCC and adjacent non-tumoral tissues from TCGA. (D, E) Evaluation of TIGDs expression in independent HCC cohorts from the international cancer genome consortium (ICGC, D) and gene expression omnibus (GEO, E) repositories. (F) Diagnostic performance of TIGDs in HCC assessed by receiver operating characteristic (ROC) curve analysis.

number.

Notably, analysis of the TCGA database revealed elevated expression of TIGD1, 3, 4, 5, 6, and 7 in hepatocellular carcinoma (HCC) tumor samples compared to normal tissues ($p < 0.001$; Fig. 1B). TIGD2 expression exhibited no statistically significant variation between HCC and normal groups. In matched specimens, levels of TIGD1, 3, 4, 5, 6, and 7 were increased in HCC relative to adjacent normal tissues, whereas TIGD2 expression was decreased in tumors ($p < 0.05$; Fig. 1C). Bioinformatics validation in the ICGC and GEO repositories further supported these findings. ICGC and GEO datasets displayed TIGDs expression profiles consistent with those from TCGA (Fig. 1D, E). In the GSE69715 cohort, differential mRNA expression between low and high TIGD4 groups did not achieve statistical significance, possibly due to the restricted sample size. Additionally, ROC analysis demonstrated strong diagnostic performance of TIGD1, 3, 5, 6, and 7 for HCC (Fig. 1F). The determined cut-off values for TIGD1 to TIGD7 were 1.025, 2.805, 0.412, 0.143, 1.645, 1.577, and 0.538, respectively.

Protein expression levels of TIGDs in HCC

Following the analysis of transcriptional expression of various TIGDs in HCC, we investigated the immunohistochemistry data on TIGDs protein expression patterns in HCC using the Human Protein Atlas (HPA) (Fig. 2). In Hepatocellular carcinoma tissues, the protein levels of TIGD1, TIGD4, TIGD6, and TIGD7 were elevated compared to the surrounding tissues, except for TIGD3 and TIGD5.

Relationship between TIGDs and clinical features

We employed the GEPIA2 database to examine the relationship of tumor staging with TIGDs (Fig. 3A). Significant variations were detected in TIGD1, TIGD4, TIGD5, TIGD6, and TIGD7 ($p < 0.05$), while TIGD3 demonstrated no statistically significant alterations. Grade 3 malignancies showed the most elevated mRNA expression for TIGD1, TIGD3, TIGD5, TIGD6, and TIGD7.

To evaluate the prognostic value of TIGDs, we performed Kaplan–Meier analyses of overall survival (OS), disease-specific survival (DSS), and progression-free interval (PFI). Using median expression as

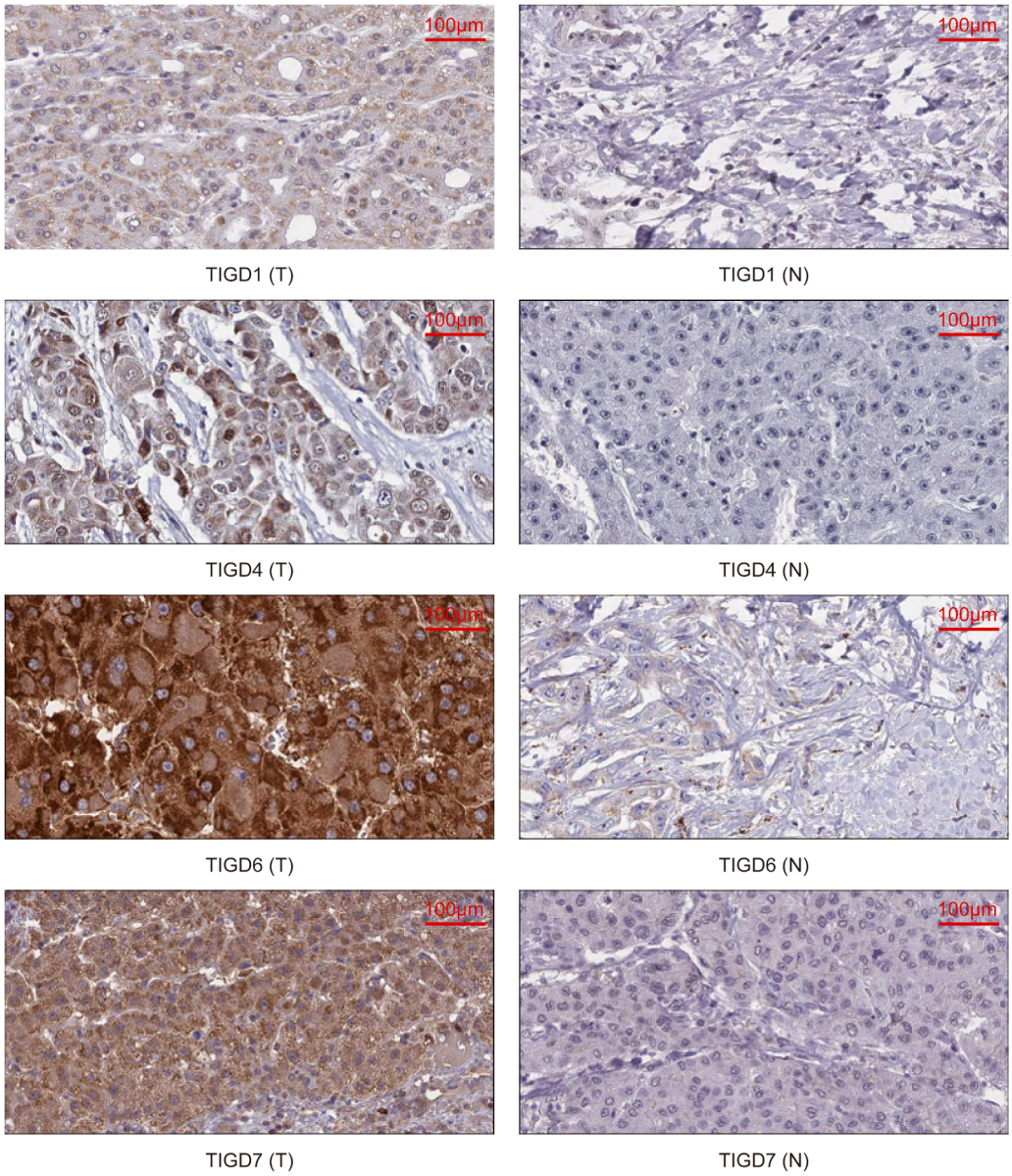

Fig. 2. Protein expression levels of TIGDs in HCC.

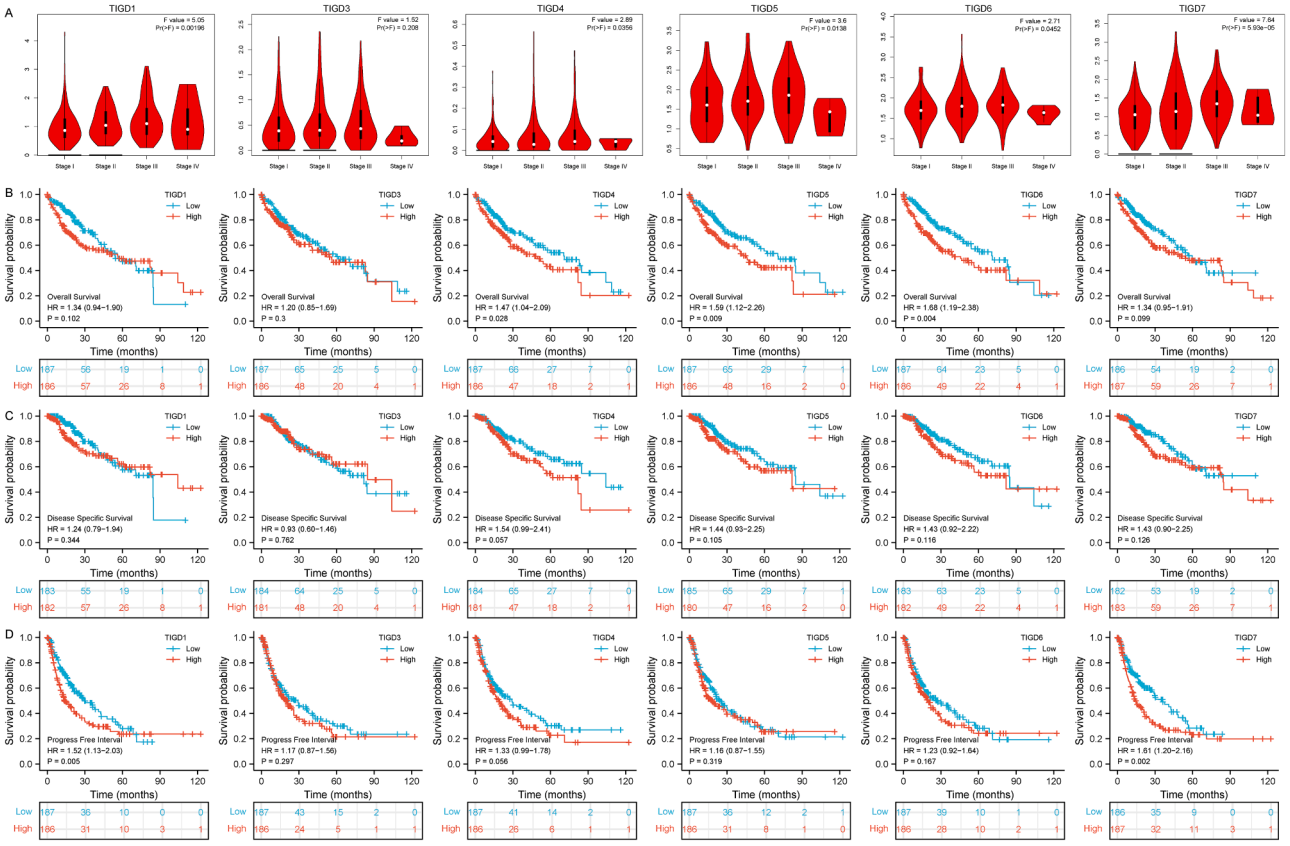

Fig. 3. (A) Relationship between TIGDs and tumor stage in HCC. Impact of TIGDs on OS (B), DSS (C), and PFI (D) in HCC.

the cutoff, hepatocellular carcinoma (HCC) patients were stratified into high- and low-expression cohorts. As shown in Fig. 3B–D, elevated expression of TIGD4, TIGD5, and TIGD6 was significantly associated with shorter OS ($p < 0.05$). TIGD4 showed a trend toward significance in relation to DSS ($p = 0.057$) and PFI ($p = 0.056$). Furthermore, high levels of TIGD1 and TIGD7 were significantly correlated with reduced PFI ($p < 0.01$). These findings suggest that TIGD4, TIGD5, and TIGD6 may serve as predictive biomarkers for survival in HCC patients.

Mutation and correlation analysis of TIGDs

Using data acquired from cBioPortal, the mutational profile of TIGDs was analyzed, indicating genetic alterations in 21.9 % of patients (80 out of 366 cases), with gene amplification representing the most frequent alteration across TIGD isoforms (Fig. 4A). In addition, TIGD5 mutations were the most commonly identified (17 %), which included amplification and missense mutations (Fig. 4C). TIGD1 harbored only amplification events, with no other mutation types detected. Genetic alternations of TIGD3 and TIGD4 included amplification, deep deletion and missense mutations. TIGD6 included amplification and truncating mutations. TIGD7 included amplification and truncating mutations.

Next, we examined the correlation among the TIGD members using the Pearson correlation analysis. As shown in Fig. 4B, significantly positive correlations were observed between TIGD1 and 3, 4, 5, 6, 7; TIGD3 and 4, 5, 6, 7; TIGD4 and 6, 7; TIGD5 and 6; TIGD6 and 7.

The relationship between TIGDs expression and immune cell infiltration

To explore potential associations between TIGD expression and the tumor immune microenvironment, we examined the correlation between TIGD levels and infiltration of 24 immune cell types in HCC using ssGSEA. While TIGDs have not been previously implicated in immune regulation, their established roles in cell cycle control and RNA splicing (Section 3.8) may indirectly influence immune cell recruitment and function. We therefore conducted an exploratory analysis to identify potential immunological correlates of TIGD expression. As illustrated in Fig. 5, TIGD1 mRNA levels demonstrated positive correlations with the infiltration of Th2 cells, NK CD56bright cells, TFH, and T helper cells ($p < 0.001$), while showing negative associations with Neutrophils, DC, Cytotoxic cells, Tgd, Mast cells, Treg, pDC, NK cells, Th17 cells, NK CD56dim cells, and CD8$^+$ T cells ($p < 0.05$). TIGD3 expression exhibited a positive association with Th2 cell infiltration ($p < 0.001$) and was inversely correlated with Neutrophils, Eosinophils, NK cells, iDC, Th17 cells, CD8$^+$ T cells, Tgd, NK CD56dim cells, DC, B cells, and Cytotoxic cells ($p < 0.05$). For TIGD4, positive correlations were observed with T helper cells, Th2 cells, Tcm, Macrophages, and aDC ($p < 0.05$), whereas negative relationships were found with pDC, Cytotoxic cells, Th17 cells, DC, and NK cells ($p < 0.05$). TIGD5 expression correlated positively with NK CD56bright cells, Th2 cells, and TFH ($p < 0.05$), and negatively with Neutrophils, DC, Th17 cells, Eosinophils, CD8$^+$ T cells, Treg, Cytotoxic cells, Tgd, pDC, and Mast cells ($p < 0.05$). TIGD6 showed a positive correlation with Tcm ($p < 0.05$) and negative correlations with Cytotoxic cells, pDC, DC, T cells, B cells, CD8$^+$ T cells, Neutrophils, NK CD56dim cells, Tem, Mast cells, and Treg ($p < 0.05$). Finally, TIGD7 expression was positively associated with Th2 cells, T helper cells, and TFH ($p < 0.05$), and negatively correlated with DC, Neutrophils, Cytotoxic cells, Tgd, pDC, iDC, B cells, Th17 cells, NK CD56dim cells, Mast cells, and T cells ($p < 0.05$). Collectively, these analyses reveal a consistent pattern of Th2-skewed immune infiltration associated with elevated TIGD expression across the TIGD family. TIGD1, TIGD3, TIGD4, TIGD5, and TIGD7 all demonstrated significant positive correlations with Th2 cell infiltration ($p < 0.001$ to $p < 0.05$), representing the most robust and reproducible immune association identified. Conversely, cytotoxic immune populations—including CD8+ *T* cells, NK cells, and cytotoxic cells—showed predominantly negative correlations with TIGD expression. This Th2-biased, cytotoxic-deficient immune profile

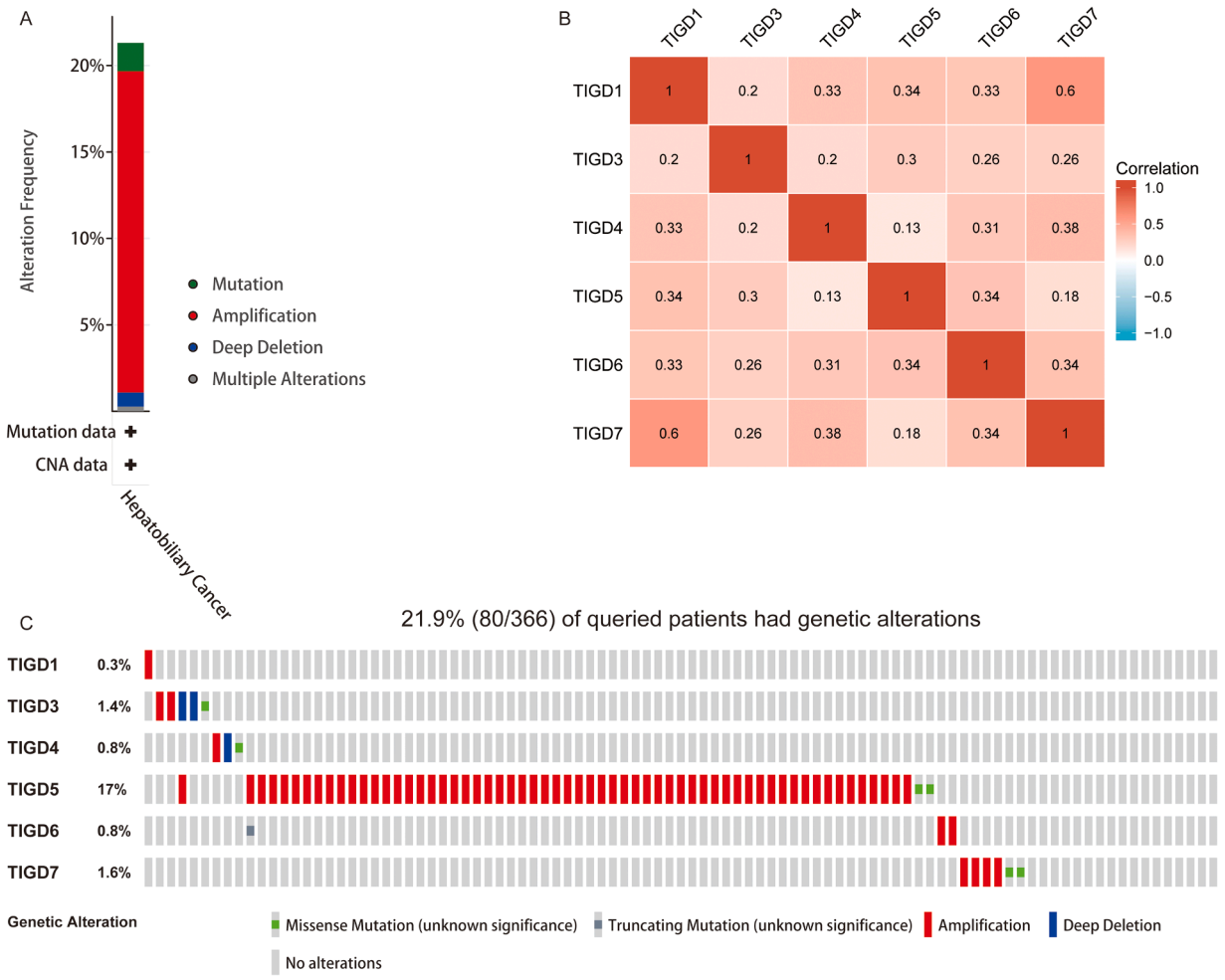

Fig. 4. presents mutational and correlational profiling of TIGDs in hepatocellular carcinoma. (A) Prevalence of mutations across TIGD isoforms. (B) Pairwise correlation analysis among TIGD family members. (C) Detailed mutational landscape for each TIGD gene across individual patient samples.

suggests that high TIGD expression may be associated with an immunosuppressive microenvironment characterized by type 2 immune polarization. The biological basis for this selective association remains unclear but may reflect TIGD-mediated effects on tumor cell proliferation (Section 3.8) that indirectly shape immune recruitment, or direct interactions between TIGD-expressing tumor cells and Th2-lineage cells that warrant experimental investigation.

Multiple immunotherapeutic approaches have demonstrated efficacy against solid tumors, notably including immune checkpoint inhibitors [37]. In recent years, therapies targeting CTLA-4 and PD-1 have shown promise as therapeutic interventions across various cancers [38]. Accordingly, we assessed TIGDs expression alongside 46 immune checkpoint-associated genes. As presented in Fig. 6, TIGD1 expression in HCC demonstrated positive correlations with 38 immune-related genes and a negative correlation with one immune-related gene ($p < 0.05$). TIGD3 exhibited positive associations with 14 immune-related genes ($p < 0.05$). Similarly, TIGD4 was positively correlated with 39 such genes ($p < 0.05$). TIGD5 showed positive correlations with 27 immune-related genes and negative correlations with 2 genes ($p < 0.05$). TIGD6 expression was positively linked to 23 immune-related genes and negatively linked to one immune gene ($p < 0.05$). For TIGD7, positive correlation was observed with 37 immune-related genes ($p < 0.05$). These associations may underlie the mechanism through which elevated TIGD4, TIGD5, and TIGD6 contribute to poor prognosis in hepatocellular carcinoma.

Cell-type-specific expression of TIGD family genes in the HCC microenvironment

Based on the methodology described, we analyzed the hepatocellular carcinoma (HCC) single-cell RNA-sequencing dataset GSE242889. After stringent quality control, dimensionality reduction, and graph-based clustering, 15 transcriptionally distinct cell clusters were identified (Fig. 7A). Cluster identities were assigned by referencing human liver-specific marker genes downloaded from the ACT database (http://xteam.xbio.top/ACT/index.jsp) and by calculating UCell enrichment scores for each cluster. The resulting annotation resolved the following cell types: dendritic cells, T cells, monocytes, endothelial cells, plasma cells, macrophages, epithelial cells, fibroblasts, B cells, and mast cells (Fig. 7B).

Comparison of cell proportions across different groups revealed that, relative to the Normal group, the proportions of fibroblasts, epithelial cells, endothelial cells, and dendritic cells were increased in the disease condition (Fig. 7C).

Expression of the six TIGD family members was visualized on UMAP embeddings (Fig. 7D–I) and further displayed via a heatmap (Fig. 7J),

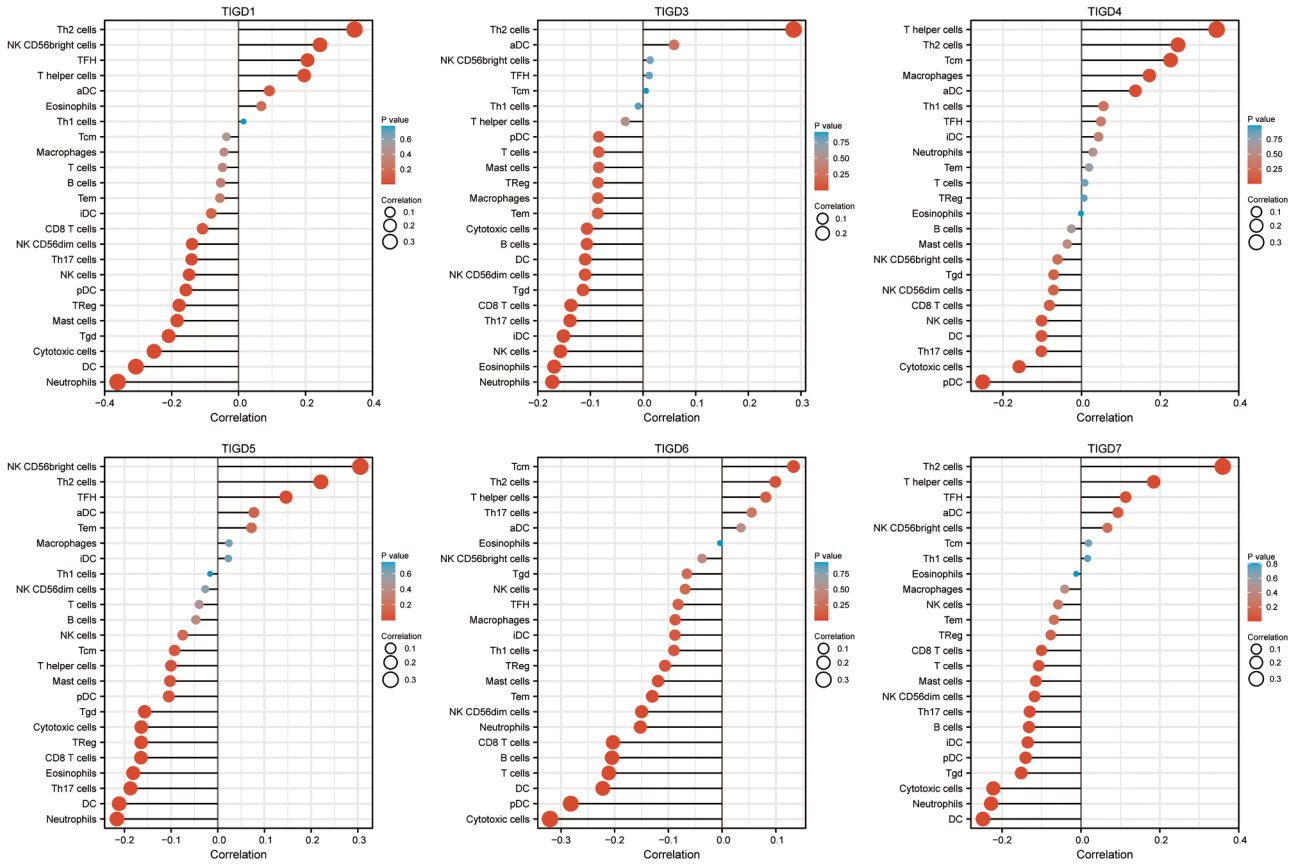

Fig. 5. Association of immune cell infiltration levels with TIGDs expression patterns.

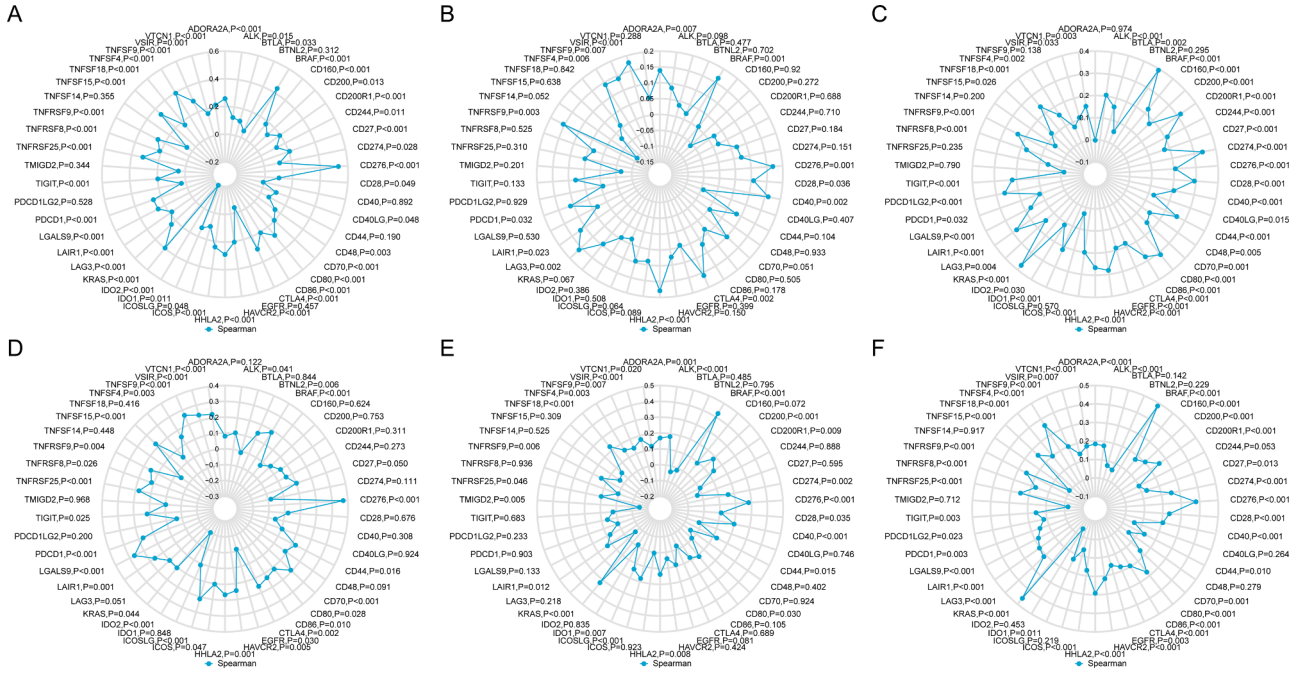

Fig. 6. Relationship between TIGDs expression levels and immune checkpoint gene profiles.

grouped heatmap (Fig. 7K), and violin plots (Fig. 7M–R). TIGD1, TIGD3, TIGD4, and TIGD6 were not expressed in mast cells but were detected in all other cell types, whereas TIGD5 and TIGD7 showed relatively high expression across all cell types.

Comparative analysis between tumor and *peri*-tumor normal tissues (multi-group differential expression volcano plot, Fig. 7L) demonstrated statistically significant upregulation of specific TIGDs in malignant microenvironment subsets: TIGD1 was elevated in tumor-derived endothelial cells; TIGD4 was downregulated in epithelial cells; TIGD5 was broadly upregulated in B cells, dendritic cells, endothelial cells,

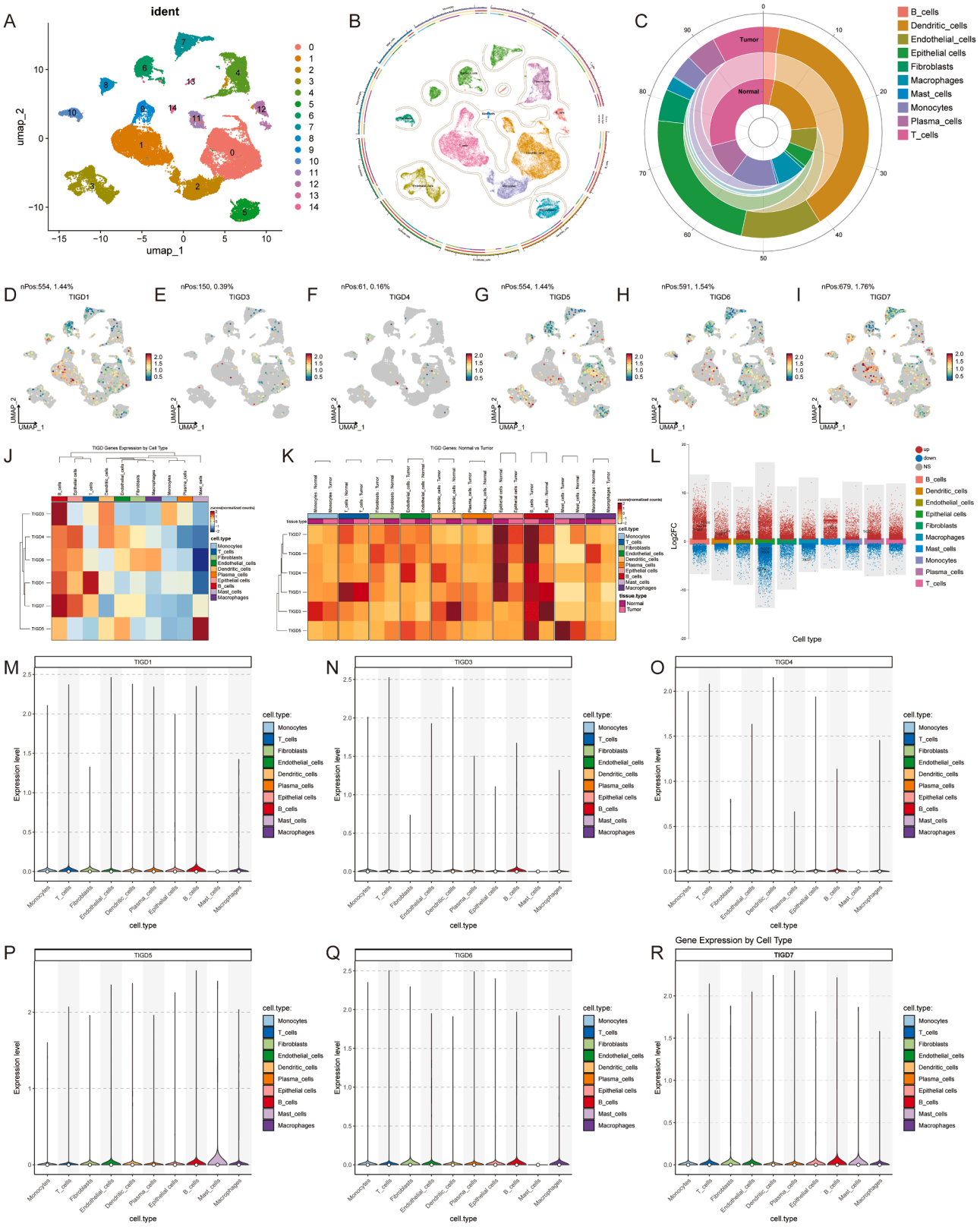

Fig. 7. Single cell expression levels of TIGDs. (A) Identification of fifteen unique cell populations derived from single-cell RNA sequencing data obtained from the dataset GSE242889, with these clusters visually represented through the application of dimensionality reduction methods. (B) The UMAP visualization displays the classification of various cell types. (C) Comparison of cell type proportions across sample groups, showing increased proportions of fibroblasts, epithelial cells, endothelial cells, and dendritic cells in the disease condition relative to the Normal group. (D-I) UMAP projections showing the expression distribution of individual TIGD family genes (TIGD1, TIGD3, TIGD4, TIGD5, TIGD6, TIGD7) across all cell types. (J) Heatmap depicting the expression levels of the six TIGD genes across the annotated cell clusters. (K) Grouped heatmap summarizing TIGD expression patterns within each major cell type. (L) Multi-group differential expression volcano plot highlighting statistically significant changes in TIGD expression between tumor and peri-tumor normal tissues across microenvironmental cell subsets. (M–R) Violin plots illustrating the expression distribution of each TIGD gene across different cell types.

mast cells, and plasma cells; TIGD6 was enriched in B cells and endothelial cells; and TIGD7 was selectively elevated in B cells and dendritic cells.

Functional characterization of TIGD5-expressing cells within the HCC tumor microenvironment

Given that TIGD5 exhibited the broadest and highest expression among tumor-infiltrating cells, we focused our functional analysis on this family member. We subsetted B cells and epithelial cells—the former representing a major TIGD5-expressing population and the latter being of particular biological interest—and performed re-annotation based on the presence or absence of TIGD5 expression (Fig. 8A). Differential expression analysis was then conducted between TIGD5+ and TIGD5- subsets for each cell type, visualized via volcano plots (Fig. 8B, C). This analysis revealed 1389 significantly upregulated and 134 downregulated genes ($|\log FC| > 1$, adj. p-value < 0.05) in TIGD5+ versus TIGD5- B cells. Similarly, TIGD5+ epithelial cells showed 1383 upregulated and 81 downregulated genes compared to their TIGD5- counterparts.

Gene Set Enrichment Analysis (GSEA) of these differentially expressed genes identified distinct activated pathways. In TIGD5+ *B* cells, enriched pathways included those related to Extracellular Matrix (ECM) organization (e.g., ECM Glycoproteins, ECM Affiliated) and growth factor signaling (e.g., FGFR2 Ligand Binding and Activation, FGFRL1 Modulation of FGFR1 Signaling, ERBB2 Activates PTK6 Signaling) (Fig. 8D). In TIGD5+ epithelial cells, pathways associated with immune regulation (Interleukin 20 Family Signaling, FceRI Mediated MAPK Activation) and pro-oncogenic signaling (Constitutive Signaling by Aberrant PI3K in Cancer, PI3K Cascade FGFR2/FGFR1) were prominently enriched (Fig. 8E).

Subsequent cell-cell communication analysis revealed a more active signaling network in tumor tissues compared to normal adjacent tissues, which exhibited a marked reduction in both the number and strength of interactions (Fig. 8F, G). Notably, within the tumor microenvironment, TIGD5+ epithelial and B cells demonstrated significantly higher interaction probability and communication strength than their TIGD5- equivalents. We focused further investigation on the enriched pathways

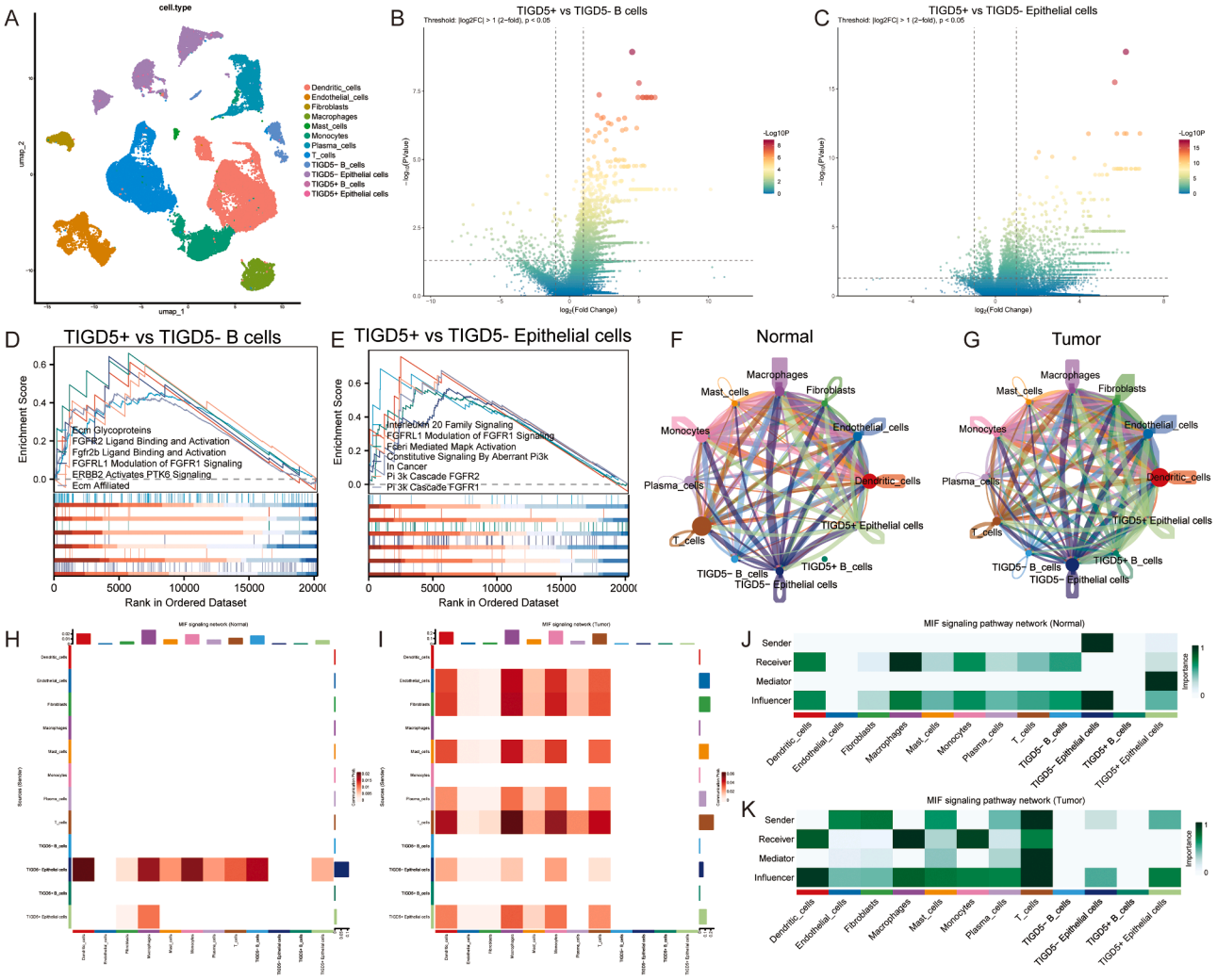

Fig. 8. Functional characterization of TIGD5-expressing cells in the HCC tumor microenvironment. (A) *Re*-annotation of B cells and epithelial cells based on the presence (TIGD5+) or absence (TIGD5−) of TIGD5 expression. (B, C) Volcano plots displaying differentially expressed genes (DEGs) between TIGD5+ and TIGD5− subsets in B cells (B) and epithelial cells (C). Thresholds: $|\log FC| > 1$, p-value < 0.05. (D, E) Gene Set Enrichment Analysis (GSEA) of DEGs from TIGD5+ vs. TIGD5− *B* cells (D) and epithelial cells (E), highlighting significantly enriched signaling pathways. (F, G) Cell-cell communication analysis comparing interaction number between tumor and normal tissues, and between TIGD5+ and TIGD5− epithelial/B-cell subsets within the tumor microenvironment. (H, I) Heatmaps depicting the sending interactions of TIGD5+ epithelial cells in normal (H) versus tumor (I) samples, with a focus on the MIF signaling pathway.
(J, K) Pathway-organized heatmaps illustrating the relative importance of different cell subsets as Senders and Influencers in MIF-mediated communication in normal (J) and tumor (K) tissues.

and the Macrophage Migration Inhibitory Factor (MIF) signaling pathway, a critical cascade in cancer progression. Heatmap visualization indicated that in tumor samples, TIGD5+ epithelial cells acted as prominent signal Senders to a wider range of target cells compared to the normal group (Fig. 8H, I). Pathway-specific analysis organized by the MIF signaling network further underscored the heightened communicative role of TIGD5+ epithelial cells in tumors, where they displayed greater importance as both Senders and Influencers (Fig. 8J, K).

Cox regression analyses of TIGD4, 5, 6 and establishment of the prognostic models for HCC

Univariate Cox regression analysis demonstrated that T stage ($p < 0.001$), tumor status ($p < 0.001$), pathologic stage ($p < 0.001$), TIGD4 ($p = 0.028$), TIGD5 ($p = 0.009$), and TIGD6 ($p = 0.004$) were associated with poor prognosis in hepatocellular carcinoma (HCC). Multivariate Cox regression identified tumor status ($p = 0.005$), TIGD5 ($p = 0.019$), and TIGD6 ($p = 0.04$) as independent prognostic factors for overall survival (OS) (Fig. 9A). Fig. 9B illustrates the distribution of TIGD4, TIGD5, and TIGD6 expression, survival status of HCC patients, and corresponding expression profiles. Blue dots indicate surviving patients, whereas red dots denote deceased individuals. The upper line corresponds to the median risk score. Areas to the left of this line designate the low-risk group, characterized by reduced TIGD4, TIGD5, and TIGD6 expression, while regions to the right represent the high-risk group with elevated expression of these genes. Progressive increases in risk scores were accompanied by a rising number of red dots and corresponding elevation in mortality rates. Collectively, these findings indicate that high-risk group patients exhibit diminished survival and heightened mortality.

Building upon earlier findings, a prognostic model for overall survival (OS) was developed by incorporating TIGD4, TIGD5, and TIGD6 mRNA expression data together with additional clinicopathological variables from the TCGA repository (Fig. 9C). Increased cumulative scores, derived from summing assigned points for individual factors in the nomogram, correlated with adverse clinical outcomes [39]. Calibration analysis evaluated the predictive accuracy of the TIGD4, TIGD5, and TIGD6 nomogram, yielding a concordance index of 0.658 for OS (Fig. 9D). The nomogram exhibited considerable clinical usefulness in estimating 1-, 3-, and 5-year survival probabilities for hepatocellular carcinoma patients.

Functional analysis of TIGDs

Following the identification of 100 genes exhibiting comparable expression profiles to TIGDs using the GEPIA2 resource, the "ClusterProfiler" (v3.14.3) R package was employed to conduct Gene Ontology (GO) and KEGG pathway enrichment studies on TIGD family members and their associated genes (Fig. 11). Three aspects of biochemical processes (BP), cellular components (CC), and molecular functions (MF) are considered in GO enrichment analysis to predict the functional roles of target host genes. GO analysis indicated that RNA splicing, mRNA metabolic process, DNA replication and cell cycle checkpoint were

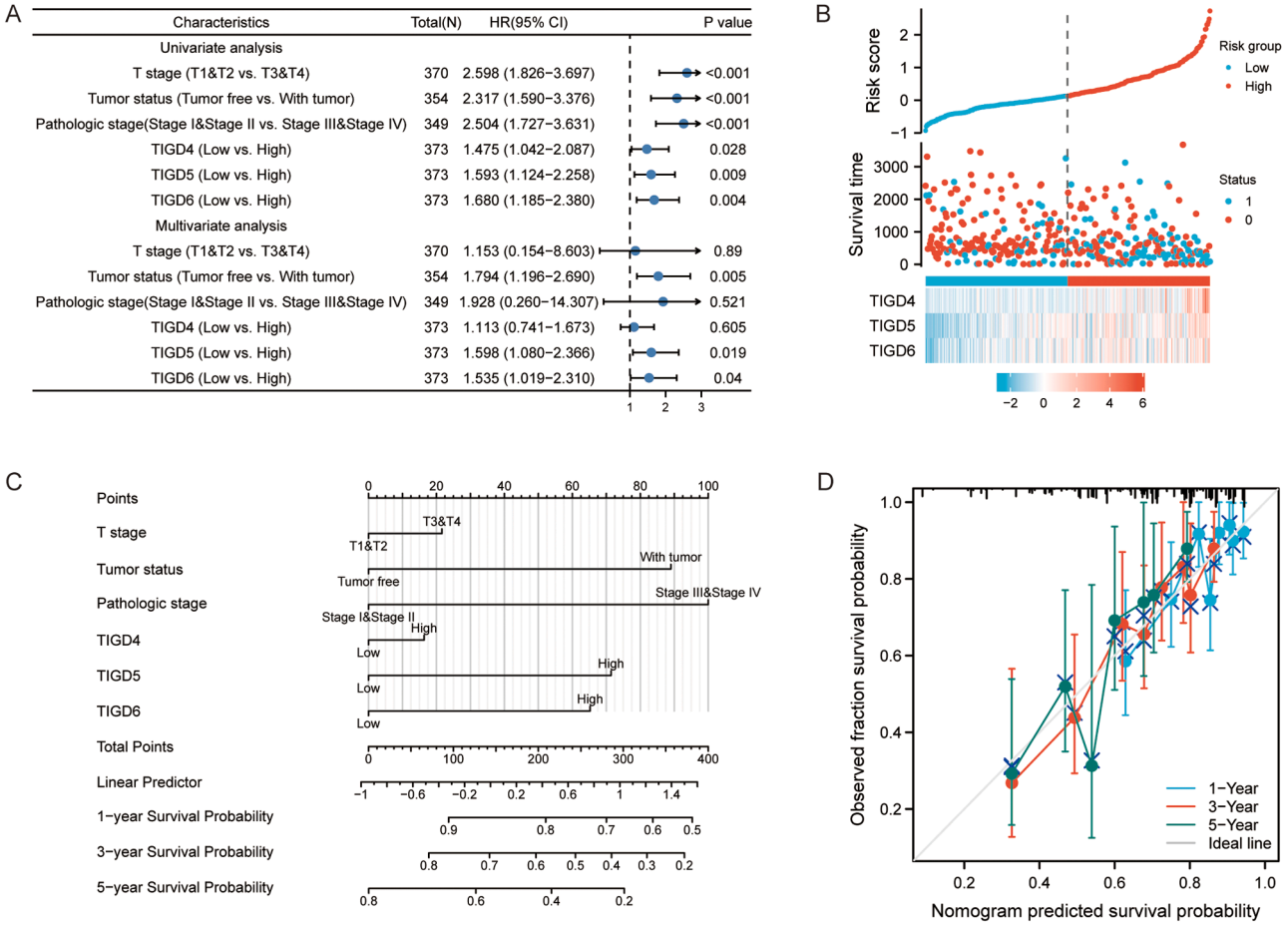

Fig. 9. Predictive significance of TIGDs expression in hepatocellular carcinoma (HCC). (A) Cox proportional hazards regression (univariate and multivariate) assessing TIGD4, TIGD5, and TIGD6 expression levels together with clinical and pathological variables. (B) Distribution of TIGD4, TIGD5, and TIGD6 expression in association with patient survival outcomes (0: deceased, 1: living). (C) Nomogram combining TIGD4, TIGD5, and TIGD6 with additional prognostic markers in HCC, derived from TCGA database. (D) Calibration plot for the nomogram's predictive accuracy.

significantly regulated by TIGDs alterations in HCC. Nuclear speck, chromosomal region, Cajal body, spliceosomal complex, catalytic step 2 spliceosome, histone acetyltransferase activity, peptide-lysine-N-acetyltransferase activity, single-stranded DNA binding, peptide N-acetyltransferase activity and N-acetyltransferase activity were also significantly controlled by these TIGDs alterations. Through KEGG analysis, pathways related to TIGDs alterations and frequently altered neighbor genes can be identified. Based on the KEGG analysis, 9 pathways were identified as being associated with TIGDs alterations in HCC. Among these pathways, spliceosome, cell cycle, homologous recombination, RNA transport and mismatch repair were involved in the tumorigenesis and pathogenesis of HCC (Figs. 10).

The mRNA relative expression of TIGD4, TIGD5 and TIGD6

Due to the statistically significant difference in overall survival rates between the low-expression and high-expression groups of TIGD4, TIGD5, and TIGD6, we selected these three genes for qPCR analysis (Fig. 11). The findings showed that TIGD5 expression varied between tumor and normal tissues. There were no notable differences in the expression of TIGD4 and TIGD6 between tumor and normal tissues, which might be attributed to the small sample size.

Discussion

This investigation performed an integrative assessment of TIGDs in hepatocellular carcinoma (HCC) patients by leveraging multiple publicly available genomic databases. Expression analyses revealed that TIGD levels in HCC tissues significantly exceeded those observed in normal liver tissues. Furthermore, elevated expression of TIGDs was consistently detected across diverse malignancies, encompassing Liver hepatocellular carcinoma (LIHC), Breast invasive carcinoma (BRCA), Cholangiocarcinoma (CHOL), Glioblastoma multiforme (GBM), Brain Lower Grade Glioma (LGG), Pancreatic adenocarcinoma (PAAD), Skin Cutaneous Melanoma (SKCM), and Thymoma (THYM). As a result of these findings, TIGDs may be able to serve as diagnostic markers in various cancers, including HCC. Furthermore, TIGD1,4,5,6,7 mRNA expression are associated with clinical stage in HCC. HCC patients expressing high levels of TIGD4, TIGD5 and TIGD6 had shorter OS than those expressing low levels, suggesting that TIGD4, TIGD5 and TIGD6 may be useful as prognostic and predictive markers. As a result, we developed a nomogram using the expression levels of TIGD4, 5, 6 along with clinical data. The nomogram provided a more precise prediction of 1-, 3-, and 5-year overall survival for HCC patients. Patients with HCC who are high-risk may benefit from the nomogram, which can be used to screen for them and determine an aggressive treatment regimen.

Additionally, the expression levels of TIGDs demonstrate associations with multiple immune checkpoint markers and diverse immune cell types. Immune infiltration, a rapidly expanding area of research, is fundamentally involved in the development and recurrence of numerous cancers. Evidence indicates that immune cells can display both anti-tumor and pro-tumor functional properties. They are recognized as pivotal elements affecting therapeutic responses and clinical outcomes post-immunotherapy [40]. Our findings indicate that TIGD family member expressions show correlations with various immune markers and the degree of immune infiltration in hepatocellular carcinoma (HCC), implying that specific TIGD family members may elucidate the immune microenvironment in HCC patients, beyond prognostic indicators.

Functional enrichment analysis revealed that TIGDs expression is linked to RNA splicing, mRNA metabolic processes, DNA replication, cell cycle checkpoints, and elevated infiltration of Th2 cells. Dysregulation of core cell-cycle components is observed in virtually all cancer types and acts as a fundamental driver of tumorigenesis [41]. Targeting the TIGD family to modulate cell cycle regulation could serve as a promising anticancer approach. Thus, our research elucidates the potential involvement of TIGDs in tumor pathogenesis and highlights their utility as biomarkers for hepatocellular carcinoma (HCC). In vitro assays further confirmed distinct TIGD5 expression patterns in tumor versus normal tissues.

TIGD1 has been reported to be a biological marker for human cancer [14].Their study found that high TIGD1 expression correlates with malignant survival in several types of cancer. It is possible that TIGD1 regulates cell-cycle progression. Our results were consistent with their observations. TIGD1 expression was notably elevated and may serve as a potential alternative therapeutic target for HCC.

TIGD3 was crucial in influencing the genome and gene evolution in both fungi and animals [24].Yao Y found that TIGD3 can be used as new biomarkers to distinguish patients with paediatric sepsis from healthy individuals [42]. Marshall OJ found that TIGD3 is most closely related to centromeric protein B (CENP-B) and localizes to the nucleus, but does not naturally bind human or mouse centromeres [43]. In our research, HCC patients at stage III exhibited the highest levels of TIGD3 expression compared to those at stages I, II, and IV.

Consistent with TIGD3, both TIGD4 and TIGD5 contribute significantly to genomic architecture and gene evolution in fungi and animals. Currently, the functional relevance of TIGD4 in hepatocellular carcinoma (HCC) remains poorly understood. Our data indicate elevated

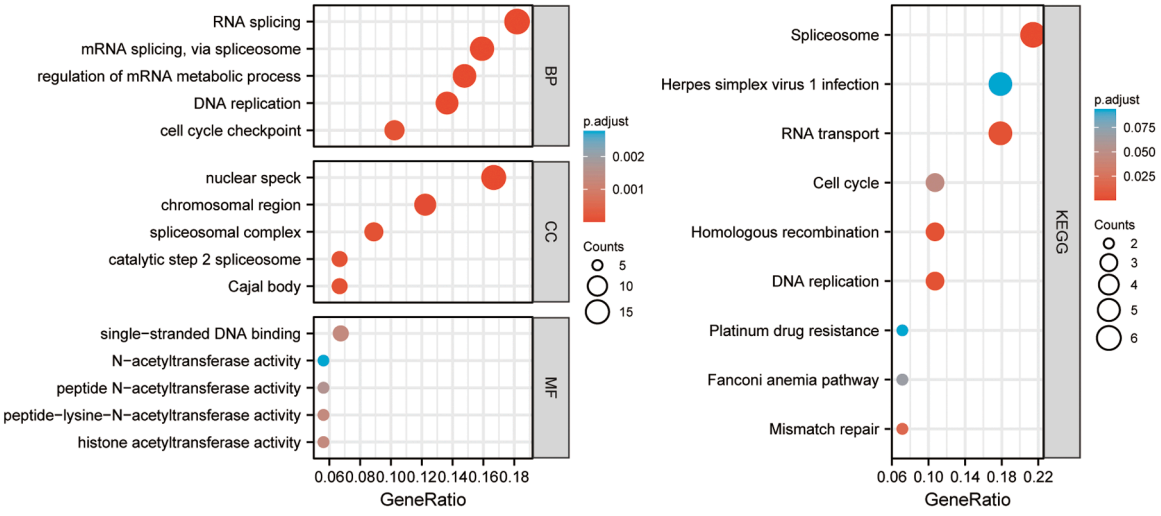

Fig. 10. GO and KEGG enrichment analysis of TIGDs.

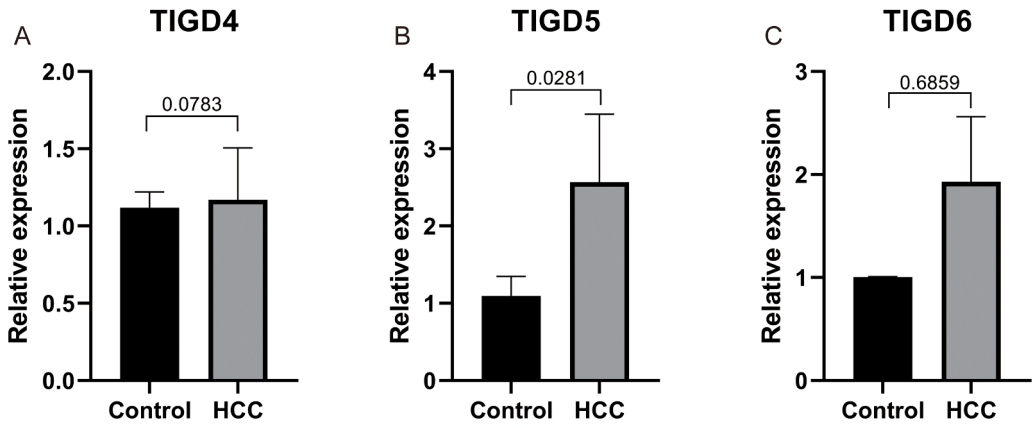

Fig. 11. The mRNA relative expression of TIGD4 (A), TIGD5 (B), TIGD6 (C).

TIGD4 mRNA expression in HCC, suggesting its potential as a therapeutic target. Utilizing the Gene Expression Omnibus database, Xu et al. identified 50 differentially expressed genes in HCC compared to normal liver tissue, among which TIGD5 was included [44]. Furthermore, TIGD5 expression was correlated with overall survival (OS) and BCLC staging. Literature on TIGD6 is currently limited. Kaewsutthi et al. detected 709 functionally significant variants displaying differential expression in obese versus control individuals, including TIGD6 [21]. To the best of our knowledge, this study represents the first comprehensive analysis of TIGD6 expression in liver cancer. Both mRNA and protein levels of TIGD6 are upregulated in HCC. Notably, TIGD4, TIGD5, and TIGD6 showed significant associations with OS. Multivariate Cox regression analysis confirmed that TIGD5 and TIGD6 serve as independent risk factors for predicting HCC prognosis.

TIGD7 encodes a protein classified within the human "tigger subfamily of the pogo superfamily of DNA-mediated transposons [45]. Previous studies have documented connections between TIGD7 and phenotypes associated with fitness [22]. Its expression shows significant correlations with alterations in body weight, fasting blood glucose, and glycosylated hemoglobin in individuals following bariatric surgery [46]. Our results further indicate that TIGD7 mRNA expression is pertinent to tumor grading, with the highest levels detected in grade III tumors. Analysis of the TCGA-LIHC cohort revealed that elevated TIGD7 expression is associated with poorer progression-free interval (PFI) compared to cases with lower expression.

Despite enhancing our comprehension of the associations involving TIGDs and hepatocellular carcinoma (HCC), several constraints inherent in this research warrant attention. First, corroboration of our data requires validation via in vitro and in vivo experimental approaches. Elucidating the functional contributions of TIGDs in HCC will necessitate the application of single-cell sequencing methodologies. In addition, the methodological framework employed here may have resulted in the oversight of other signaling mechanisms associated with TIGDs.

Conclusion

In summary, TIGD1, 3, 4, 5, 6, 7 mRNA expressions were overexpressed in HCC. Our findings suggest that the TIGD family plays a significant role in HCC, with TIGD4, TIGD5, and TIGD6 serving as potential prognostic and predictive markers. Enrichment analysis demonstrated that TIGDs may function as oncogenic drivers via modulation of cell cycle control, RNA splicing mechanisms, and mRNA metabolic pathways. Our findings identify TIGD4, TIGD5, and TIGD6 as candidate biomarkers for hepatocellular carcinoma (HCC) diagnosis and prognosis, emphasizing their relevance as possible targets for immunotherapeutic interventions.

Availability of data and materials

The data produced and examined in this study can be requested from the corresponding author if needed. Additionally, raw data is freely accessible from online databases such as TCGA, HPA, cBioPortal, ICGC, GEO, and GEPIA2.

Funding

This study was supported by Ningxia Natural Science Foundation (2025AAC030449 and 2025AAC030421).

Ethics statement

This study was conducted in accordance with the Declaration of Helsinki and was approved by the Ethics Committee of People's Hospital of Ningxia Hui Autonomous Region (approval number: [2025]-NZR-243).

Consent for publication

Not applicable.

CRediT authorship contribution statement

Jing Liu: Writing – review & editing, Data curation. **Xiaopeng Chen:** Writing – review & editing, Writing – original draft. **Cheng Liu:** Writing – original draft. **Chengwei Yang:** Writing – original draft, Data curation. **Baoding Li:** Writing – review & editing.

Declaration of competing interest

There are no conflicts of interest regarding the publication of this article.

Acknowledgements

We acknowledge the TCGA, HPA, cBioPortal, ICGC, GEO and GEPIA2 databases for free use.

References

[1] C. Tang, C. He, D. Wang, J. Guo, X. Yin, H. Ye, L. Wu, Y. Zhang, S. Zeng, X. Zeng, et al., Co-delivery of sorafenib and an FSP1 inhibitor triggers dual ferroptosis in tumor cells and immunosuppressive macrophages for enhanced immunotherapy in mouse models of hepatocellular carcinoma, Nat. Commun. 16 (1) (2025) 10096, https://doi.org/10.1038/s41467-025-65056-9. From NLM.

[2] J. Wang, X. Chen, D. Wu, C. Jia, Q. Lian, Y. Pan, J. Yang, Single-cell and machine learning approaches uncover intrinsic immune-evasion genes in the prognosis of

hepatocellular carcinoma, Liver. Res. 8 (4) (2024) 282–294, https://doi.org/10.1016/j.livres.2024.11.001. From NLM.
[3] M.J. Moschitto, P.F. Doubleday, D.S. Catlin, N.L. Kelleher, D. Liu, R.B. Silverman, Mechanism of inactivation of ornithine aminotransferase by (1S,3S)-3-amino-4-(hexafluoropropan-2-ylidenyl)cyclopentane-1-carboxylic acid, J. Am. Chem. Soc. 141 (27) (2019) 10711–10721, https://doi.org/10.1021/jacs.9b03254. From NLM.
[4] X. Huo, S. Jiang, S. Wu, Q. Lian, H. Chen, Mechanosensitive ion channel-related genes in hepatocellular carcinoma: unraveling prognostic genes and their roles in drug resistance and immune modulation, Liver Res. 9 (1) (2025) 36–48, https://doi.org/10.1016/j.livres.2025.01.002. From NLM.
[5] F. Yang, Q. Lian, B. Ni, X. Qiu, Y. He, X. Zou, F. He, W. Chen, MUTYH is a potential prognostic biomarker and correlates with immune infiltrates in hepatocellular carcinoma, Liver Res. 6 (4) (2022) 258–268, https://doi.org/10.1016/j.livres.2022.12.002. From NLM.
[6] J. Zhuo, H. Li, P. Zhang, C. He, W. Shen, X. Yang, Z. Lin, R. Zhuang, X. Wei, S. Zheng, et al., Growth differentiation factor 7 alleviates the proliferation and metastasis of hepatocellular carcinoma, Liver Res. 8 (4) (2024) 259–268, https://doi.org/10.1016/j.livres.2024.09.006. From NLM.
[7] F. Yang, B. Ni, Q. Lian, X. Qiu, Y. He, Q. Zhang, X. Zou, F. He, W. Chen, Key genes associated with non-alcoholic fatty liver disease and hepatocellular carcinoma with metabolic risk factors, Front. Genet. 14 (2023) 1066410, https://doi.org/10.3389/fgene.2023.1066410. From NLM.
[8] F. Wang, S.J.P. Breslin, W. Qiu, Novel oncogenes and tumor suppressor genes in hepatocellular carcinoma, Liver Res. 5 (4) (2021) 195–203, https://doi.org/10.1016/j.livres.2021.06.001. From NLM.
[9] F. Chen, Q. Li, X. Xu, F. Wang, Clinical characteristics and risk factors of hepatitis B virus-related cirrhosis/hepatocellular carcinoma: a single-center retrospective study, Liver Res. 7 (3) (2023) 237–243, https://doi.org/10.1016/j.livres.2023.07.004. From NLM.
[10] W. Abdelhamed, M. El-Kassas, Hepatitis B virus as a risk factor for hepatocellular carcinoma: there is still much work to do, Liver Res. 8 (2) (2024) 83–90, https://doi.org/10.1016/j.livres.2024.05.004. From NLM.
[11] J. Tu, B. Wang, X. Wang, K. Huo, W. Hu, R. Zhang, J. Li, S. Zhu, Q. Liang, S. Han, Current status and new directions for hepatocellular carcinoma diagnosis, Liver Res. 8 (4) (2024) 218–236, https://doi.org/10.1016/j.livres.2024.12.001. From NLM.
[12] T. Dou, S. Gu, Z. Zhou, C. Ji, L. Zeng, X. Ye, J. Xu, K. Ying, Y. Xie, Y. Mao, Isolation and characterization of a Jerky and JRK/JH8 like gene, tigger transposable element derived 7, TIGD7, Biochem. Genet. 42 (7–8) (2004) 279–285, https://doi.org/10.1023/b:bigi.0000034428.95802.35. From NLM.
[13] B. Gao, Y. Wang, M. Diaby, W. Zong, D. Shen, S. Wang, C. Chen, X. Wang, C. Song, Evolution of pogo, a separate superfamily of IS630-Tc1-mariner transposons, revealing recurrent domestication events in vertebrates, Mob. DNA 11 (2020) 25, https://doi.org/10.1186/s13100-020-00220-0. From NLM.
[14] Y. Yang, G. Liu, L. Qin, L. Ye, F. Zhu, Y. Ying, Overexpression of UHRF1 and its potential role in the development of invasive ductal breast cancer validated by integrative bioinformatics and immunohistochemistry analyses, Transl. Cancer Res. 8 (4) (2019) 1086–1096, https://doi.org/10.21037/tcr.2019.06.19. From NLM.
[15] X. Ge, Z. Liu, X. Jiao, X. Yin, X. Wang, G. Li, Establishment and validation of a gene signature-based prognostic model to improve survival prediction in adrenocortical carcinoma patients, Int. J. Endocrinol. 2021 (2021) 2077633, https://doi.org/10.1155/2021/2077633. From NLM.
[16] J. Prahl, G.A. Coetzee, Genetic elements at the Alpha-synuclein locus, Front. Neurosci. 16 (2022).
[17] D.M. van Leeuwen, R.W. Gottschalk, G. Schoeters, N.A. van Larebeke, V. Nelen, W. F. Baeyens, J.C. Kleinjans, J.H. van Delft, Transcriptome analysis in peripheral blood of humans exposed to environmental carcinogens: a promising new biomarker in environmental health studies, Environ. Health Perspect. 116 (11) (2008) 1519–1525, https://doi.org/10.1289/ehp.11401. From NLM.
[18] Mamoor, S. TIGD4 is differentially expressed in the lymph node metastases of patients with breast cancer. 2021.
[19] H.-J. Schulten, M. Bangash, S. Karim, A. Dallol, D. Hussein, A. Merdad, F.K. Al-Thoubaity, J. Al-Maghrabi, A. Jamal, F. Al-Ghamdi, Comprehensive molecular biomarker identification in breast cancer brain metastases, J. Transl. Med. 15 (1) (2017) 1–20.
[20] X. Xie, L. Li, H. Wu, F. Hou, Y. Chen, Q. Xue, Y. Zhou, J. Zhang, J. Gong, R. Song, Comprehensive integrative analyses identify TIGD5 rs75547282 as a risk variant for Autism spectrum disorder, Autism Res. 14 (4) (2021) 631–644.
[21] S. Kaewsutthi, J. Santiprabhob, B. Phonrat, A. Tungtrongchitr, P. Lertrit, R. Tungtrongchitr, Exome sequencing in Thai patients with familial obesity, Genet. Mol. Res. 15 (2016) 8311.
[22] E. Rampersaud, L. Nathanson, J. Farmer, K. Meshbane, R.L. Belton, A. Dressen, M. Cuccaro, A. Musto, S. Daunert, S. Deo, Genomic signatures of a global fitness index in a multi-ethnic cohort of women, Ann. Hum. Genet. 77 (2) (2013) 147–157.
[23] T. Dou, S. Gu, Z. Zhou, C. Ji, L. Zeng, X. Ye, J. Xu, K. Ying, Y. Xie, Y. Mao, Note: isolation and characterization of a jerky and JRK/JH8 like gene, Tigger transposable element derived 7, TIGD7, Biochem. Genet. 42 (7) (2004) 279–285.
[24] B. Gao, Y. Wang, M. Diaby, W. Zong, D. Shen, S. Wang, C. Chen, X. Wang, C. Song, Evolution of pogo, a separate superfamily of IS630-Tc1-mariner transposons, revealing recurrent domestication events in vertebrates, Mob. DNA 11 (1) (2020) 1–15.
[25] Q. Guo, X. Zhong, Z. Dang, B. Zhang, Z. Yang, Identification of GBN5 as a molecular biomarker of pan-cancer species by integrated multi-omics analysis, Discover Oncol. 16 (1) (2025) 85, https://doi.org/10.1007/s12672-025-01840-9. From NLM.
[26] T. Lu, Y. Zheng, X. Gong, Q. Lv, J. Chen, Z. Tu, S. Lin, J. Pan, Q. Guo, J. Li, High expression of hyaluronan-mediated motility receptor predicts adverse outcomes: a potential therapeutic target for head and neck squamous cell carcinoma, Front. Oncol. 11 (2021) 499.
[27] Z. Tang, B. Kang, C. Li, T. Chen, Z. Zhang, GEPIA2: an enhanced web server for large-scale expression profiling and interactive analysis, Nucleic Acids Res. 47 (W1) (2019) W556–W560.
[28] F. Pontén, K. Jirström, M. Uhlen, The Human Protein Atlas—a tool for pathology, J. Pathol. J. Pathol. Soc. G. B. Irel. 216 (4) (2008) 387–393.
[29] Gu, Z. cBioPortal. 2016.
[30] Q. Liu, Q. Lian, Y. Song, S. Yang, C. Jia, J. Fang, Identification of LSM family members as potential chemoresistance predictive and therapeutic biomarkers for gastric cancer, Front. Oncol. 13 (2023) 1119945, https://doi.org/10.3389/fonc.2023.1119945. From NLM.
[31] S. Hänzelmann, R. Castelo, J. Guinney, GSVA: gene set variation analysis for microarray and RNA-seq data, BMC Bioinform. 14 (2013) 1–15.
[32] G. Bindea, B. Mlecnik, M. Tosolini, A. Kirilovsky, M. Waldner, A.C. Obenauf, H. Angell, T. Fredriksen, L. Lafontaine, A. Berger, Spatiotemporal dynamics of intratumoral immune cells reveal the immune landscape in human cancer, Immunity. 39 (4) (2013) 782–795.
[33] Q. Lian, C. Ma, X. Wang, J. Wang, J. Zeng, J. Zhang, Y. Li, Serglycin's role in primary liver cancer: insights into tumor microenvironment and macrophage interaction, Front. Immunol. 16 (2025) 1668627, https://doi.org/10.3389/fimmu.2025.1668627. From NLM.
[34] L. Li, X. Lu, Q. Lian, X. Wang, C. Jia, C. Xu, Apoptotic vesicles of mesenchymal stem cells promote M2 polarization and alleviate early-onset preeclampsia via miR-191-5p, Stem Cell Res. Ther. 16 (1) (2025) 414, https://doi.org/10.1186/s13287-025-04546-5. From NLM.
[35] F. Quan, X. Liang, M. Cheng, H. Yang, K. Liu, S. He, S. Sun, M. Deng, Y. He, W. Liu, et al., Annotation of cell types (ACT): a convenient web server for cell type annotation, Genome Med. 15 (1) (2023) 91, https://doi.org/10.1186/s13073-023-01249-5. From NLM.
[36] Q. Guo, X. Xu, X. Li, Y. Mao, S. Li, Y. Yao, X. Li, Y. Li, J. Feng, Y. Shu, et al., Assessing the relationships of 1400 blood metabolites with abdominal aortic aneurysm: a Mendelian randomization study, Front. Pharmacol. 15 (2024) 1514293, https://doi.org/10.3389/fphar.2024.1514293. From NLM.
[37] A. Karachi, F. Dastmalchi, D.A. Mitchell, M. Rahman, Temozolomide for immunomodulation in the treatment of glioblastoma, Neuro Oncol. 20 (12) (2018) 1566–1572.
[38] F. Xu, H. Lin, P. He, L. He, J. Chen, L. Lin, Y. Chen, A TP53-associated gene signature for prediction of prognosis and therapeutic responses in lung squamous cell carcinoma, Oncoimmunology 9 (1) (2020) 1731943.
[39] Y. Kim, G.A. Margonis, J.D. Prescott, T.B. Tran, L.M. Postlewait, S.K. Maithel, T. S. Wang, D.B. Evans, I. Hatzaras, R. Shenoy, Nomograms to predict recurrence-free and overall survival after curative resection of adrenocortical carcinoma, JAMA Surg. 151 (4) (2016) 365–373.
[40] J. Li, Z. Xu, L. Zhou, K. Hu, Expression profile and prognostic values of chromobox family members in human glioblastoma, Aging 14 (4) (2022) 1910.
[41] J.M. Suski, M. Braun, V. Strmiska, P. Sicinski, Targeting cell-cycle machinery in cancer, Cancer Cell 39 (6) (2021) 759–778.
[42] Y. Yao, J. Zhao, J. Hu, H. Song, S. Wang, Y. Wang, Identification of a four-gene signature for diagnosing paediatric sepsis, Biomed. Res. Int. (2022) 2022.
[43] O.J. Marshall, K. Choo, Putative CENP-B paralogues are not present at mammalian centromeres, Chromosoma 121 (2) (2012) 169–179.
[44] W. Xu, Q. Rao, Y. An, M. Li, Z. Zhang, Identification of biomarkers for Barcelona Clinic Liver Cancer staging and overall survival of patients with hepatocellular carcinoma, PLoS. One 13 (8) (2018) e0202763.
[45] M. Martínez-Bueno, M.E. Alarcón-Riquelme, Exploring impact of rare variation in systemic lupus erythematosus by a genome wide imputation approach, Front. Immunol. 10 (2019) 258.
[46] S.Z. Berisha, D. Serre, P. Schauer, S.R. Kashyap, J.D. Smith, Changes in whole blood gene expression in obese subjects with type 2 diabetes following bariatric surgery: a pilot study, PLoS. One 6 (3) (2011) e16729.